Towards a Predictive Behavioural Model for Service Robots in Shared Environments

Alessandro Antonucci and Daniele Fontanelli

***Abstract*— Service robots are increasingly applied in real life environments populated with human beings. In such a challenging scenario, the autonomous robots have to avoid collision in a "natural" way, that is to execute trajectories that a human would follow. This challenging goal can be efficiently tackled if a sufficiently descriptive human motion model is available, in order to predict future pedestrian behaviour and hence safely planning the correct route. In this paper, we move a first step towards a motion model that is able to describe to a certain extent the nonverbal negotiation of spaces in shared environments, still preserving its simplicity for ease of computation. The avoidance task is shared among the robot and the pedestrians and thus human-like trajectories can be generated. Simulations and application to actual pedestrian data are presented to validate the model.**

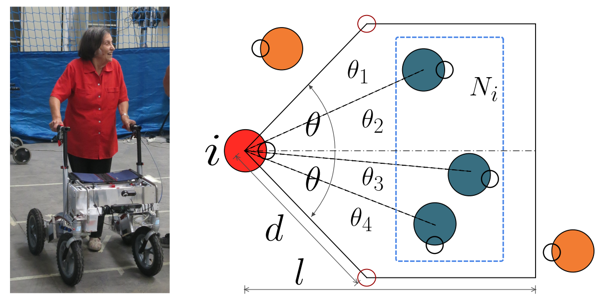

(a) (b)

Fig. 1. (a) The *FriWalk* with a senior. (b) IPS shape according to [2], with characteristic sizes, and the neighbours for pedestrian i. *Blue* pedestrians are inside the IPS at time t, so they belongs to $N_i(t)$, *orange* ones are out of scope.

I. Introduction

One of the main problems for ground service robots that is currently asking for affordable and effective solutions is the synthesis of safe motions in environments shared with human beings. In this context, collision avoidance trajectories to ensure a safe human interaction are becoming an aspect of particular relevance in order to let robots to navigate with a human-like behaviour that persons can easily interpret [1], [2], [3]. An example of this kind is given by the European project ACANTO [4], where the *FriWalk* (see Figure 1-a), a standard commercial walking aid endowed with sensing abilities to understand the surroundings and localise in the environment [5], [6], [7], with guidance abilities to drive the user in the surroundings [8], [9], [10] and with planning abilities to produce safe paths in the environment [11], [12], is used as a navigation aid for seniors. One of the most important features of the *FriWalk* is its ability to respond to unforeseen events along the execution of the planned path, such as the presence of bystanders or walking pedestrians. To this end, predictive models are considered. The current reactive planner [13], [14] running on the *FriWalk* is based on the Headed Social Force Model (HSFM) [15], an extended version of the rather famous Social Force Model [16] that explicitly considers the pedestrians' heading to increase its modelling potentialities. The limit of such an approach is that the avoidance manoeuvre is currently entirely responsibility of the robot, while the human is assumed to be completely unaware [13], [14].

This project has received funding from the European Unions Horizon 2020 Research and Innovation Programme - Societal Challenge 1 (DG CONNECT/H) under grant agreement n° 643644 "ACANTO - A CyberphysicAl social NeTwOrk using robot friends"

The authors are with the Department of Industrial Engineering (DII), University of Trento, Via Sommarive 5, Trento, Italy daniele.fontanelli@unitn.it

This paper lays down the main conceptual modelling aspects to be applied on the planning or reactive control for a service robot, which the *FriWalk* is the most immediate application example. The idea is to propose a computationally simple predictive model (in order to be executed online on-board the available embedded computing platforms) that catches the action and reaction behaviour of nonverbal humans' space negotiation for effective and more "natural" reactive collision-avoidance behaviours. The proposed Predictive Headed Social Force Model (PHSFM) implements a geometric method able to improve the *reactive* approach of common social force models and additionally implement a *predictive* behaviour. In fact, pedestrians don't simply react to interactions with neighbours, but actively predict the most appropriate way to avoid collisions respecting others personal spaces [17].

This paper is organised as follows. Section II presents a detailed analysis of the state of the art. Section III gives an overview and explains the rationale of the model proposed in this paper, while Section IV precisely discusses its details. The results based on the proposed model are offered in Section V and Section VI, where both simulations and validation analyses on actual pedestrian data are reported. Finally, in Section VII we summarise the benefits and the novelties of the proposed model, together with concluding remarks and future research directions.

II. Related work

There are two main approaches for human motion prediction: learning and reasoning. In learning-based techniques, e.g. [3], predictions are grounded on observations. Despite the proven effectiveness of learning-based methods, almost all of these methods require extensive off-line training and consequently the variety of the behaviours that can be emulated is limited by the size of the database. In reasoning (or model)-based prediction, e.g. [18], the behaviour is determined on a-priori assumptions on geometric considerations and typical motion velocity. A simple, yet not effective, way to predict human motion is by using a linear model where human trajectories are formed by mostly straight lines, as used in Velocity Obstacle (VO) local planner [19], [20], where avoidance manoeuvres are planned by selecting the robot velocities outside the velocity-based "collision cone". Although computationally efficient, it is unclear whether humans do follow model-based precise geometric rules. In particular, the force parameters often need to be tuned individually, and can vary significantly for different pedestrians.

Several model-based solutions adopt the SFM [16] due to its simplicity and effectiveness (see for instance [11]). However, adopting the SFM as is does not prevent collisions between agents [21]. In particular, [22] pointed out that the presence of reactive forces in the SFM leads pedestrians only to passively avoid collisions, which generates unnatural behaviours, to account for they propose an optimal problem. To incorporate an anticipatory behaviour in the SFM, velocity-based approaches were introduced: for instance, [23] uses a power-law interaction that is also based not on the physical separation between pedestrians and on their projected time to a potential future collision. The perception of the relative motion of neighbour obstacles is performed considering the *time-to-collision* also in [24], in which the agents are simulated by minimising the risk of collision.

Previous research on human behaviour helps identifying key factors affecting human avoidance, among which proxemics is one of the most popular and widely accepted [25]. Following the hypothesis of a reciprocal interaction between two colliding pedestrians, [17] found a temporal structure of three successive phases: *observation* of the collision, avoidance *reaction*, and path *regulation*. Moreover, it showed that human beings adapt their trajectory collaboratively, but the one giving way (i.e. the second at the crossing) deviates more than the one passing first. Path adjustments seemed to be independent by the head rotation or walking speed, whereas speed adjustments were influenced by different walking speed [26]. These findings support the assumption of path adjustments as a default collision avoidance strategy in the presence of sufficient space and justify the choices made for the PHSFM presented next.

III. Predictive Headed Social Force Model

Avoidance mechanism cannot be represented as a reactive action, because force-based models try to describe motion directly from the observed movements of pedestrians, ignoring the internal cognitive processes that lead to the movements [22]. To improve force-based models, such as the SFM or the HSFM, an agent is modelled so as to move in a direction in which there are no obstacles, reducing the deviations from the direct path to its destination [22], [27], [28].

In our model we mimic the avoidance manoeuvres performed by pedestrians by directly modifying the desired speed $\mathbf{v}_i^d$ that in the HSFM model points towards the final goal. This way, we explicitly compute what is the local walking direction that pedestrians are supposed to choose, so instead of being rejected by their neighbours, as happens in the SFM, they actively seek a free path in order to avoid collisions. Possible collisions are classified in two general types, namely *passing case* and *crossing case*. Each simulated agent searches for both present and future obstacles inside his Information Process Space (IPS) [2], computing also the *time-to-collision*.

The IPS (Figure 1-b) does not coincide with the personal space, which instead is a circular-shaped area around the person used to identify collisions with other pedestrians [25]. Passing case occurs when two or more pedestrians walk along parallel trajectories; this situation is identified if other people are present in the IPS or if a collision with another pedestrian will occur within a time limit. For this case we adopt the same formulation of [22]; however, we also consider the repulsive forces of the SFM, since they are essential to represent the elementary avoidance between pedestrians. Crossing case occurs when pedestrian walk along crossing trajectories, that is in our model when the closest neighbour among those present in IPS has a direction such that it passes through the IPS middle line. In such a case, the idea is to assign the desired walking directions of two interacting agents (robot and human), by computing the effort that each agent puts in order to avoid the collision. This asymmetrical behaviour, first proposed in [29] using reinforcement learning, is obtained using geometrical arguments. Our work constructs a similar function using the HSFM as a baseline and parametrises this feature with the minimum number of relevant factors, i.e. the bearing angle and the two pedestrians' velocities.

IV. Model description

In this section, we first summarise the HSFM [15], and then we derive the new added features for the passing and crossing cases, respectively.

A. HSFM

The HSMF improves the SMF with the inclusion of pedestrians' heading to better model the human motion behaviour when not heavily populated environments are considered [15]. The position and the velocity of the i-th individual with mass m_i and radius r_i, expressed in the global reference frame $\langle W \rangle$, are respectively denoted by $\mathbf{r}_i = [x_i, y_i]^T$ and $\mathbf{v}_i = [\dot{x}_i, \dot{y}_i]^T$. The equations of motion according to the SFM are simply $\dot{\mathbf{r}}_i = \mathbf{v}_i$ and $\dot{\mathbf{v}}_i = \frac{1}{m_i}\mathbf{u}_i$, where $\mathbf{u}_i$ represent the social force driving the i-th particle. In order to model the pedestrians heading, it's convenient to attach a body frame $\langle B \rangle$ to each individual, i.e. a reference frame centred at the pedestrians position and whose x-axis is aligned with the pedestrians forward direction of motion. Let $\mathbf{q}_i = [\theta_i, \omega_i]^T$ be the vector containing the heading θ_i (angle between the x-axis of the body frame and that of the global reference frame) and the angular velocity $\omega_i = \dot{\theta}_i$ of the i-th pedestrian. Denote by $\mathbf{v}_i^B = [v_i^f, v_i^o]^T$ the velocity vector expressed in the body frame. The components v_i^f and v_i^o of vector $\mathbf{v}_i^B$ correspond to the projection of the velocity vector $\mathbf{v}_i$ along the forward direction and the orthogonal direction, respectively. Clearly, $\mathbf{v}_i = \mathbf{R}(\theta_i)\mathbf{v}_i^B$, where the 2D rotation matrix $\mathbf{R}(\theta_i)$ of angle θ_i is defined as

$$\mathbf{R}(\theta_i) = \begin{bmatrix} \cos(\theta_i) & -\sin(\theta_i) \\ \sin(\theta_i) & \cos(\theta_i) \end{bmatrix} = \begin{bmatrix} \mathbf{r}_i^f \, \mathbf{r}_i^o \end{bmatrix}. \tag{1}$$

Then the human locomotion model becomes

$$\begin{aligned} \dot{\mathbf{r}}_i &= \mathbf{R}(\theta_i)\mathbf{v}_i^B, \\ \dot{\mathbf{v}}_i^B &= \frac{1}{m_i}\mathbf{u}_i^B, \\ \dot{\mathbf{q}}_i &= \begin{bmatrix} 0 & 1 \\ 0 & 0 \end{bmatrix} \mathbf{q}_i + \begin{bmatrix} 0 \\ \frac{1}{I_i} \end{bmatrix} u_i^\theta, \end{aligned} \tag{2}$$

where I_i denotes the moment of inertia of pedestrian i. In the model (2), the control inputs are $\mathbf{u}_i^B = [u_i^f, u_i^o]^T$, with u_i^f is the force acting along the forward direction and u_i^o the force along the orthogonal direction, as well as the torque u_i^θ about the axis perpendicular to the plane of motion. In this model, if we set $v_i^o(t) = 0$ in $\mathbf{v}_i^B$ and $u_i^o(t) = 0$ in $\mathbf{u}_i^B$, for all t, the dynamic unicycle model is recovered, hence the model features a nonholonomic behaviour. The HSFM models the control inputs u_i^f , u_i^o and u_i^θ on the basis of external forces. The total force $\mathbf{f}_i$ that acts on the i-th pedestrian is defined as $\mathbf{f}_i = \mathbf{f}_i^o + \mathbf{f}_i^e$. The first term accounts for the pedestrians desire to move with a given velocity vector $\mathbf{v}_i^d = v_i^d \mathbf{e}_i^d$, i.e.

$$\mathbf{f}_i^o = m_i \frac{\mathbf{v}_i^d - \mathbf{v}_i}{\tau_i}, \tag{3}$$

where the characteristic time $\tau_i > 0$ parameter determines the rate of change of the velocity vector, v_i^d and $\mathbf{e}_i^d$ are the desired velocity and the vector toward the desired goal of pedestrian i. The second term $\mathbf{f}_i^e$ is the sum of the forces generated by the environment, e.g. fixed obstacles, walls, furnitures, etc., and other pedestrians in the environments. A natural choice for computing u_i^f is to project $\mathbf{f}_i$ along the forward direction, while u_i^o is computed by projecting only the interaction force $\mathbf{f}_i^e$ along the orthogonal to the pedestrian heading, scaled by a gain parameter $k^o > 0$. Moreover, in order to drive to zero the sideward velocity v_i^o when the sideward force is zero, a damped dynamic proportional to v_i^o is added to u_i^o with a damping parameter $k^d > 0$. The input u_i^θ has a second order dynamic depending on the constants $k^\lambda > 0$ and $\alpha^\lambda > 1$ shaping its rate of convergence towards the desired heading. Forces are obtained as in the SFM [16].

B. Passing case

We define $N_i(t)$ as the set of pedestrians inside the IPS of pedestrian i at time t, namely the *neighbours*. If nobody is inside the IPS, we search the ones that will enter in the personal space d_{per_i} of pedestrian i (i.e. collide) within a time window $t < t' < t + T_c$, being T_c the maximum time

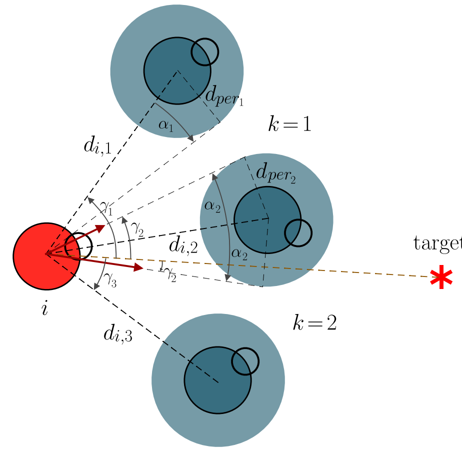

Fig. 2. Illustration of desired velocities v_i^{set} (*red vectors*) for passing case with two gaps k.

for an interaction between agents. So pedestrian i will collide with the pedestrian j when

$$\left\| \mathbf{r}_j(t) - \mathbf{r}_i(t) - \left(\mathbf{v}_j(t) - \mathbf{v}_i^{\mathrm{d}}\right)(t' - t) \right\| \leq d_{per_i}. \tag{4}$$

Their positions at the collision will be the *collision points* and, when happening inside the IPS, we have $j \in N_i(t)$. The lines joining the pedestrian i and his neighbours together with the IPS angular limits form a set of angles $\theta_k(t)$ (Figure 1-b). If no occlusion between pedestrian occurs, the number of angles is equal to the cardinality of $N_i(t) + 1$.

Pedestrian i can choose one slot between two adjacent neighbours to go through when his original walking direction is obstructed. If we treat the gap between two neighbours as a bottleneck, we can make an assumption that the desired velocity decreases as the gap narrows [22]; pedestrians than can walk freely with velocity $\mathbf{v}_i^{\mathrm{d}}$ when the gap is bigger than a threshold ϑ_u and almost stop if the latter becomes below ϑ_l. According to [28], the relation between desired velocity v_i^{d} and the sector is an s-curve function (with parameters α_p and β_p)

$$\overline{v}_i^{\mathrm{D}}(t) = \frac{v_i^{\mathrm{d}}}{1 + \exp\left[\left(\alpha_p - \vartheta_k(t)\right)/\beta_p\right]}, \tag{5}$$

where $\vartheta_k(t)$

$$\begin{aligned} \vartheta_k(t) = &-d_{per_k} - d_{per_{k+1}} + \\ &+ \sqrt{d_{i,k}^2(t) + d_{i,k+1}^2(t) - 2 d_{i,k}(t) d_{i,k+1}(t) \cos(\theta_k(t))}, \end{aligned} \tag{6}$$

models the size of the gap, and $d_{i,k}(t)$ and $d_{i,k+1}(t)$ are the distances from pedestrian i to the neighbours k and $k+1$.

The angle between the segment joining pedestrians i and k and the segment connecting pedestrian i and the goal (i.e. the direct path) is dubbed $\gamma_k(t)$ (see Figure 2). We assume that pedestrian i will choose for every gap a specific direction according to his target position and the personal spaces of his neighbours. If the target is directly reachable using the gap k, no deviation angle is imposed, i.e. $\eta_k(t) = 0$. If it is reachable but the angle $\gamma_k(t)$ (or $\gamma_{k+1}(t)$) is smaller then the hindrance angle $\alpha_k = \arcsin\left(\frac{d_{per_k}}{d_{i,k}(t)}\right)$, which is the projection of neighbour's k personal space seen by pedestrian i, we impose a direction at least tangential to that personal space, i.e. $\eta_k(t) = \gamma_k(t) + \alpha_k$. If the target is not reachable from the gap k, we directly impose on pedestrian i to pass close to the nearest neighbour k w.r.t. the target, i.e. $\eta_k(t) = \gamma_k(t) + \alpha_k$, because pedestrians do not want to deviate too much from the direct path [28].

Since pedestrians want to get to their destination as soon as possible, we finally assume that they will choose the direction in which the projection of their velocity to the direct path is the maximum. Hence, the following simple discrete optimisation problem is defined:

$$\begin{aligned} \arg\max_k \quad & v_i^{set}(\theta_k(t)), \\ \text{s.t.} \quad & v_i^{set}(\theta_k(t)) = \overline{v}_i^{\mathrm{D}}(t)\cos\eta_k(t), \end{aligned} \tag{7}$$

whose solution k^* gives immediately the modulus $v_i^{set}(\theta_{k^*}(t))$ and phase $\angle\mathbf{e}_i^d + \eta_{k^*}(t)$ of the desired velocity $\mathbf{v}_i^d(t)$ to be used in the HSFM.

C. Crossing case

In a crossing case, the nearest pedestrian j in $N_i(t)$ will pass in the middle of pedestrian i's IPS, assuming a constant velocity motion. Inspired by [29], first we identify who's going to pass in front and who's going to give way, and then we compute the avoidance manoeuvres. To this end, we compute the *crossing point* time for both the pedestrians, defined by $t_i = d_i/|\mathbf{v}_i|$, $t_j = d_j/|\mathbf{v}_j|$, where d_i and d_j are the distances from the crossing point. Notice that this is not a collision point but, instead, a geometric point that allows both pedestrians to pass untouched along their current trajectories (Figure 3-a). Then, we find the bearing angle β, which is the angle between the segment joining the pedestrian i to the crossing point and the segment joining i and j, positive if pedestrian j is on the left of pedestrian i. The bearing angle and the crossing times are used over a generalised logistic function to find the *sharing effort coefficient* α, defined as

$$\alpha(t) = \operatorname{sign}(\beta)\operatorname{sign}(t_i - t_j)\frac{1}{1+\exp\left[-c\left(t_i - t_j\right)\right]}, \tag{8}$$

where c is the steepness coefficient. This function, depicted in Figure 3-b, describes how $\alpha(t)$ may span from 1 (maximum deviation) to 0 (no deviation at all) depending on the difference in time between the agents. The rationale is the following: the more time until the crossing, the lower the deviation from the direct path is. When times are equal, both pedestrians have a coefficient of 0.5. Hence, for $\alpha(t)$ ranging from 0.5 to 1, pedestrian is going to give away to the other: if so, a deviation angle

$$\eta(t) = \alpha(t)\eta_{max}b^{t_i}, \tag{9}$$

is chosen to pass behind the other pedestrian, where η_{max} is the maximun deviation angle and b is the decreasing factor. The sign of $\alpha(t)$ determines the left/right side for deviation (see also Figure 3). Notice that for $\alpha(t)$ ranging from 0 to 0.5, the pedestrian is going to pass first, hence the deviation

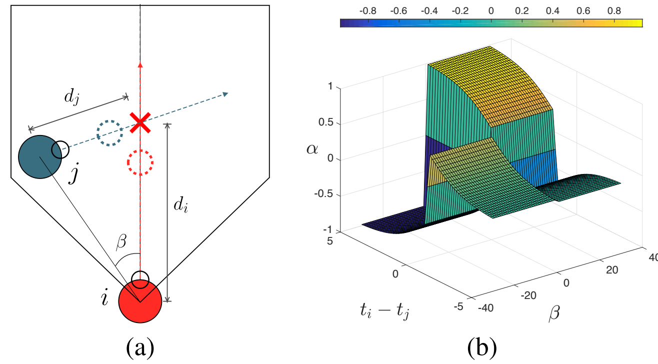

Fig. 3. (a) Illustration of crossing case. *Red mark* is the crossing point, the *dashed circles* are the pedestrian's collision points. (b) Sharing effort coefficient function, with bearing angle β in degree and crossing order.

will be smaller and of the opposite sign of the pedestrian giving the way (that has $\alpha(t)$ between 0.5 to 1). The absolute orientation will be $\angle\mathbf{e}_i^d + \eta(t)$. The pedestrian giving the way also changes the velocity value following the s-curve function

$$\overline{v}_i^{\mathrm{D}}(t) = \frac{v_i^{\mathrm{d}}}{1+\exp\left[\left(\alpha_c - t_i\right)/\beta_c\right]}, \tag{10}$$

which directly depends on the time to the crossing point t_i. Despite its simplicity, these geometric-based rules are quite effective in modelling the negotiation of the space in the shared environment.

V. Simulation results

In this section, we first present the results of the simulations of the PHSFM with synthesised trajectories for the passing and the crossing cases. To better highlight the effectiveness of the proposed model in reproducing specific evasive manoeuvres performed by pedestrians, we present a comparison with the SFM and the HSFM. The parameters related to the dynamic model of pedestrians in (2) have been chosen coherently as reported in [15], except for $k^\lambda = 0.02$, which generates smoother trajectories. The radius r_i of each pedestrian has been set to 0.3 [m], while mass m_i have been randomly generated in the intervals $[60, 90]$ [kg]. Based on the evidence coming from real data (see Section VI), we have set $d_{per} = 0.8$ [m] and $T_c = 3$ [s]. The IPS parameters were set to $d = 2.5$ [m], $\theta = 45°$ and $l = 3.5$ [m] (see Figure 1-b). The length is adequate for large and fairly crowded environment, while the angular aperture is robust to some typical phenomena, such as lane formation or individuals moving in groups (which is not explicitly considered in this first version of the model). According to these values, we set $\alpha_p = 1$, $\beta_p = 0.2$ of (5) in order to have free desired velocity for a gap greater than $\vartheta_u = 1.5$ [m] (with $\vartheta_l = 0.5$ [m]) and a small but non-zero velocity at the origin. The crossing case instead requires that in the worst case pedestrian i is able to stop (hence s/he will stop for $t_i < 1$ [s]), while he can walk freely for $t_i > T_c$. For the s-curve function (10), we have chosen $\alpha_c = 1.5$ and $\beta_c = 0.2$, while $c = 0.8$ in (8), and $\eta_{max} = 45°$ and $b = 0.2$ in (9).

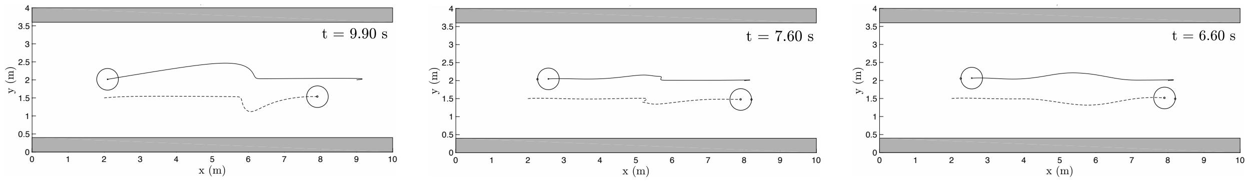

(a) (b) (c)

Fig. 4. Corridor scenario: (a) Social Force Model, (b) HSFM, (c) PHSFM.

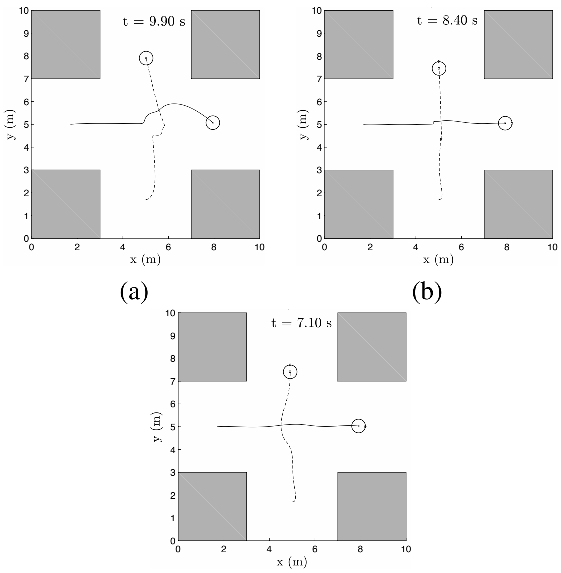

(a) (b) (c)

Fig. 5. Intersecting corridors scenario: (a) Social Force Model, (b) HSFM, (c) PHSFM.

The two different scenarios are the corridor (Figure 4) for the passing case and the intersecting corridors (Figure 5) for the crossing case. In the interest of comparison, only two pedestrians per simulation are considered. From the reported trajectories, it is evident how the SFM generates in this specific scenario unnatural bouncing trajectories (Figure 4-a), while for the HSFM (Figure 4-b) this effect is mitigated, but the pedestrians do not account for the reciprocal behaviour. In the PHSFM case (Figure 4-c), the possible collision is perceived in advance and a smooth avoidance manoeuvre is accomplished by both the pedestrians, according to the behaviour described in Section IV-B.

Similar results are obtained in the intersecting corridors case in Figure 5. Under the forces of the SFM, the agents reciprocally push each other away (Figure 5-a), while thanks to the persons' orientation, the HSFM generate more compliant trajectories (Figure 5-b). In Figure 5-c the shared avoidance is exhibited, with the pedestrian moving vertically that successfully avoid the other giving the way, while the other shows a small path adjustment according to the shared effort coefficient, as described in Section IV-C.

VI. Validation on real data

To validate the PHSFM with actual trajectories traveled by pedestrians in urban environments, and, again, to compare it with the SFM and the HSFM, we conducted simulations comparing the generated trajectories with the dataset from [30], [31], [32]. The selected datasets respectively include motion capture of hand-labelled pedestrians' trajectories for two environments: a controlled experiment at the Instituto Tecnológico de Buenos Aires (ITBA) and a corridor in a shopping center in Japan. In the interest of space, we report only the results with the dataset [30], being the other results similar. The prediction accuracy depends to a large extent on the simulation parameters, which are a function also of the environment. Therefore, all the parameters are the same of Section V, except for $r_i = 0.25$ [m], $d = 1.5$ [m], $\theta = 45°$, $l = 2$ [m], $k^{\lambda} = 0.2$ and $\eta_{max} = 45°$, $b = 0.2$ for the passing case, or $\eta_{max} = 80°$, $b = 0.5$ for the crossing case. For a qualitative analysis, Figure 6 reports examples of interactions captured from the dataset: both the actual and simulated trajectories are reported. Notice how the HSFM has a stiffer behaviour that the PHSFM, which is also evident in the crossing case, not reported here due to space limits. This is mainly due to the unmodelled action and reaction negotiation of the pedestrian. From a quantitative view-point, the mean errors of the two models, computed for each agent as the error in position between the predicted trajectory and the actual trajectory at the same time instant, are substantially the same. However, the maximum error is slightly better for the HSFM. Nonetheless, the possibility of modelling the action and reaction becomes a clear advantage for the passing case, in both qualitative and quantitative terms.

VII. Conclusion

In this work, we have presented a new human motion model based on the well-known Social Force Model. A collision prediction phase and a geometric method to represent evasion manoeuvres performed by pedestrians during interactions in shared spaces has been applied on top of the HSFM, hence the name Predictive HSFM. The validation of the model has been demonstrated throughout a set of simulations and comparisons with real-life human trajectories in urban environments. Future research directions will focus on the application of the model to reactive planning algorithms in a stochastic framework, that is when the possible action and reaction manoeuvres are weighted by a certain degree of confidence. Another important improvement is related to the extension to social groups of human beings walking together.

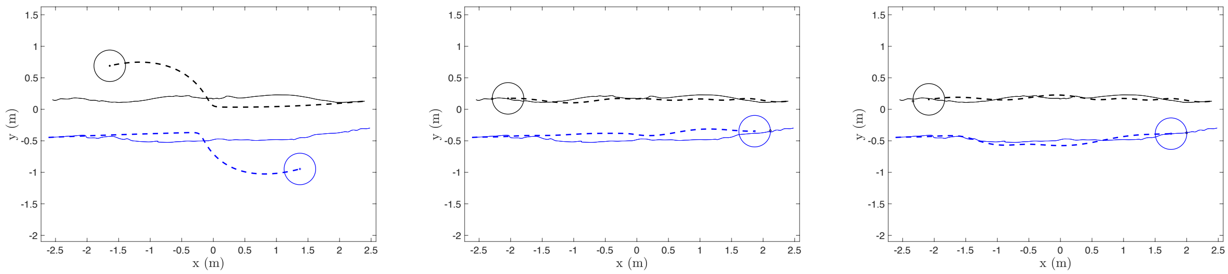

(a) (b) (c)

Fig. 6. First example: (a) SFM, (b) HSFM and (c) PHSFM. Both actual trajectories (solid lines, from [30]) and predicted trajectories (dashed lines) are reported.

REFERENCES

[1] K. Charalampous, I. Kostavelis, and A. Gasteratos, "Recent trends in social aware robot navigation: A survey," *Robotics and Autonomous Systems*, 2017.

[2] J. Rios-Martinez, A. Spalanzani, and C. Laugier, "From proxemics theory to socially-aware navigation: A survey," *International Journal of Social Robotics*, vol. 7, no. 2, pp. 137–153, 2015.

[3] T. Kruse, A. K. Pandey, R. Alami, and A. Kirsch, "Human-aware robot navigation: A survey," *Robotics and Autonomous Systems*, vol. 61, no. 12, pp. 1726–1743, 2013.

[4] "ACANTO: A CyberphysicAl social NeTwOrk using robot friends," http://www.ict-acanto.eu/acanto, February 2015, EU Project.

[5] V. Magnago, L. Palopoli, R. Passerone, D. Fontanelli, and D. Macii, "A Nearly Optimal Landmark Deployment for Indoor Localisation with Limited Sensing," in *International Conference on Indoor Positioning and Indoor Navigation (IPIN)*. Sapporo, Japan: IEEE, Sept. 2017, pp. 1–8.

[6] P. Nazemzadeh, D. Fontanelli, D. Macii, and L. Palopoli, "Indoor Localization of Mobile Robots through QR Code Detection and Dead Reckoning Data Fusion," *IEEE Trans. on Mehcatronics*, 2017, available on line.

[7] P. Nazemzadeh, F. Moro, D. Fontanelli, D. Macii, and L. Palopoli, "Indoor Positioning of a Robotic Walking Assistant for Large Public Environments," *IEEE Trans. on Instrumentation and Measurement*, vol. 64, no. 11, pp. 2965–2976, Nov 2015.

[8] M. Andreetto, S. Divan, D. Fontanelli, and L. Palopoli, "Harnessing Steering Singularities in Passive Path Following for Robotic Walkers," in *Proc. IEEE International Conference on Robotics and Automation (ICRA)*. Singapore: IEEE, May 2017, pp. 2426–2432.

[9] M. Andreetto, S. Divan, F. Ferrari, D. Fontanelli, L. Palopoli, and F. Zenatti, "Simulating passivity for Robotic Walkers via Authority-Sharing," *IEEE Robotics and Automation Letters*, vol. 3, no. 2, pp. 1306–1313, April 2018.

[10] M. Andreetto, S. Divan, D. Fontanelli, and L. Palopoli, "Path Following with Authority Sharing between Humans and Passive Robotic Walkers Equipped with Low-Cost Actuators," *IEEE Robotics and Automation Letters*, vol. 2, no. 4, pp. 2271–2278, Oct. 2017.

[11] A. Colombo, D. Fontanelli, A. Legay, L. Palopoli, and S. Sedwards, "Efficient customisable dynamic motion planning for assistive robots in complex human environments," *Journal of Ambient Intelligence and Smart Environments*, vol. 7, no. 5, pp. 617–633, 2015.

[12] L. Palopoli, A. Argyros, J. Birchbauer, A. Colombo, D. Fontanelli, *et al.*, "Navigation Assistance and Guidance of Older Adults across Complex Public Spaces: the DALi Approach," *Intelligent Service Robotics*, vol. 8, no. 2, pp. 77–92, 2015.

[13] P. Bevilacqua, M. Frego, E. Bertolazzi, D. Fontanelli, L. Palopoli, and F. Biral, "Path Planning maximising Human Comfort for Assistive Robots," in *IEEE Conference on Control Applications (CCA)*. Buenos Aires, Argentina: IEEE, Sept. 2016, pp. 1421–1427.

[14] P. Bevilacqua, M. Frego, D. Fontanelli, and L. Palopoli, "Reactive Planning for Assistive Robots," *IEEE Robotics and Automation Letters*, vol. 3, no. 2, pp. 1276–1283, April 2018.

[15] F. Farina, D. Fontanelli, A. Garulli, A. Giannitrapani, and D. Prattichizzo, "Walking ahead: The headed social force model," *PloS one*, vol. 12, no. 1, p. e0169734, 2017.

[16] D. Helbing and P. Molnar, "Social force model for pedestrian dynamics," *Physical review E*, vol. 51, no. 5, p. 4282, 1995.

[17] A.-H. Olivier, A. Marin, A. Crétual, A. Berthoz, and J. Pettré, "Collision avoidance between two walkers: Role-dependent strategies," *Gait & posture*, vol. 38, no. 4, pp. 751–756, 2013.

[18] D. Althoff, D. Wollherr, and M. Buss, "Safety assessment of trajectories for navigation in uncertain and dynamic environments," in *Robotics and Automation (ICRA), 2011 IEEE International Conference on*. IEEE, 2011, pp. 5407–5412.

[19] J. Van Den Berg, J. Snape, S. J. Guy, and D. Manocha, "Reciprocal collision avoidance with acceleration-velocity obstacles," in *Robotics and Automation (ICRA), 2011 IEEE International Conference on*. IEEE, 2011, pp. 3475–3482.

[20] D. Zhang, Z. Xie, P. Li, J. Yu, and X. Chen, "Real-time navigation in dynamic human environments using optimal reciprocal collision avoidance," in *Mechatronics and Automation (ICMA), 2015 IEEE International Conference on*. IEEE, 2015, pp. 2232–2237.

[21] M. Luber, J. A. Stork, G. D. Tipaldi, and K. O. Arras, "People tracking with human motion predictions from social forces," in *Robotics and Automation (ICRA), 2010 IEEE International Conference on*. IEEE, 2010, pp. 464–469.

[22] W. Qian-Ling, C. Yao, D. Hai-Rong, Z. Min, and N. Bin, "A new collision avoidance model for pedestrian dynamics," *Chinese Physics B*, vol. 24, no. 3, p. 038901, 2015.

[23] I. Karamouzas, B. Skinner, and S. J. Guy, "Universal power law governing pedestrian interactions," *Physical review letters*, vol. 113, no. 23, p. 238701, 2014.

[24] T. B. Dutra, R. Marques, J. B. Cavalcante-Neto, C. A. Vidal, and J. Pettré, "Gradient-based steering for vision-based crowd simulation algorithms," in *Computer Graphics Forum*, vol. 36, no. 2. Wiley Online Library, 2017, pp. 337–348.

[25] E. T. Hall, *The hidden dimension: man's use of space in public and private*. Bodley Head, 1969.

[26] M. Huber, Y.-H. Su, M. Krüger, K. Faschian, S. Glasauer, and J. Hermsdörfer, "Adjustments of speed and path when avoiding collisions with another pedestrian," *PloS one*, vol. 9, no. 2, p. e89589, 2014.

[27] A. V. Savkin and C. Wang, "Seeking a path through the crowd: Robot navigation in unknown dynamic environments with moving obstacles based on an integrated environment representation," *Robotics and Autonomous Systems*, vol. 62, no. 10, pp. 1568–1580, 2014.

[28] M. Moussaïd, D. Helbing, and G. Theraulaz, "How simple rules determine pedestrian behavior and crowd disasters," *Proceedings of the National Academy of Sciences*, vol. 108, no. 17, pp. 6884–6888, 2011.

[29] J. G. Da Silva Filho and T. Fraichard, "Human robot motion: A shared effort approach," in *European Conference on Mobile Robotics*, 2017.

[30] D. R. Parisi, P. A. Negri, and L. Bruno, "Experimental characterization of collision avoidance in pedestrian dynamics," *Physical Review E*, vol. 94, no. 2, p. 022318, 2016.

[31] A. Robicquet, A. Sadeghian, A. Alahi, and S. Savarese, "Learning social etiquette: Human trajectory understanding in crowded scenes," in *European conference on computer vision*. Springer, 2016, pp. 549–565.

[32] F. Zanlungo, T. Ikeda, and T. Kanda, "Potential for the dynamics of pedestrians in a socially interacting group," *Physical Review E*, vol. 89, no. 1, p. 012811, 2014.